Nancolas, B., & Halestrap, A. (2016). The anti-tumour agent lonidamine is a potent inhibitor of the mitochondrial pyruvate carrier and plasma membrane monocarboxylate transporters. Biochemical Journal, 473, 929-936. DOI: 10.1042/BJ20151120

The anti-tumour agent lonidamine is a potent inhibitor of the mitochondrial pyruvate carrier and plasma membrane monocarboxylate transporters

Bethany Nancolas[1], Lili Guo[3], Rong Zhou[2], Kavindra Nath[2], David S. Nelson[2], Dennis B. Leeper[4], Ian A. Blair[3], Jerry D. Glickson[2] and Andrew P. Halestrap[1]

[1]School of Biochemistry, Biomedical Sciences Building, University of Bristol, BS8 1TD, UK.
[2]Laboratory of Molecular Imaging, B6 Blockley Hall, Department of Radiology, University of Pennsylvania School of Medicine, Philadelphia, PA 19104, USA
[3]Penn Superfund Research and Training Program Center, Center of Excellence in Environmental Toxicology, and Department of Systems Pharmacology and Translational Therapeutics, University of Pennsylvania School of Medicine, Philadelphia, PA, 19104, USA
[4]Department of Radiation Oncology, Thomas Jefferson University, Philadelphia, PA 19107, USA.
Corresponding Author: Andrew P Halestrap (A.Halestrap@Bristol.ac.uk)

Short title: Lonidamine inhibition of the MPC and MCTs

Key words: cancer, metabolism, bioenergetics, tumour acidification, monocarboxylate transporter, mitochondrial pyruvate carrier.

Summary Statement
The mode of action of lonidamine, an established anti-tumour drug, remains controversial. We show that lonidamine potently inhibits the mitochondrial pyruvate carrier and plasma membrane monocarboxylate transporters, accounting for many of its known effects on tumour cell metabolism and bioenergetics.

ABSTRACT

Lonidamine (LND) is an anti-tumour drug particularly effective at selectively sensitising tumours to chemotherapy, hyperthermia and radiotherapy, although its precise mode of action remains unclear. It has been reported to perturb the bioenergetics of cells by inhibiting glycolysis and mitochondrial respiration, while indirect evidence suggests it may also inhibit L-lactic acid efflux from cells mediated by members of the proton-linked monocarboxylate transporter (MCT) family and also pyruvate uptake into the mitochondria by the mitochondrial pyruvate carrier (MPC). Here we test these possibilities directly. We demonstrate that LND potently inhibits MPC activity in isolated rat liver mitochondria (K_i 2.5 μM) and cooperatively inhibits L-lactate transport by MCT1, MCT2 and MCT4 expressed in *Xenopus laevis* oocytes with $K_{0.5}$ and Hill Coefficient values of 36-40 μM and 1.65-1.85. In rat heart mitochondria LND inhibited the MPC with similar potency and uncoupled oxidation of pyruvate was inhibited more effectively (IC_{50} ~7 μM) than other substrates including glutamate (IC_{50} ~20 μM). In isolated DB-1 melanoma cells 1-10 μM LND increased L-lactate output, consistent with MPC inhibition, but higher concentrations (150 μM) decreased L-lactate output while increasing intracellular [L-lactate] > five-fold, consistent with MCT inhibition. We conclude that MPC inhibition is the most sensitive anti-tumour target for LND, with additional inhibitory effects on MCT-mediated L-lactic acid efflux and glutamine/glutamate oxidation. Together these actions can account for published data on the selective tumour effects of LND on L-lactate, intracellular pH (pHi) and ATP levels that can be partially mimicked by the established MPC and MCT inhibitor α-cyano-4-hydroxycinnamate.

Abbreviations used

AR-C155858, 6-[(3,5-Dimethyl-1H-pyrazol-4-yl)methyl]-5-[[(4S)-4-hydroxy-2-isoxazolidinyl]carbonyl]-3-methyl-1-(2-methylpropyl)thieno[2,3-d]pyrimidine-2,4(1H,3H)-dione; CHC, α-cyano-4-hydroxycinnamate; IC_{50}, Inhibitor concentration giving 50% inhibition; ISB, Isolation buffer; LND, Lonidamine; MCT, Monocarboxylate Transporter; MPC, Mitochondrial Pyruvate Carrier; PCA, Perchloric acid; pHi, Intracellular pH; DIPEA, ethyldiisopropylamine.

INTRODUCTION

Lonidamine (LND), first introduced in 1979 as an antispermadocidic agent [1], has limited antineoplastic activity as a single agent [2;3], but has exceptional potential in modulating the activities of conventional chemotherapeutic agents such as N-mustards [4;5], anthracyclines [4;6] and temozolomide [7], as well as hyperthermia [8;9], radiation therapy [10;11] and photodynamic therapy [12]. LND also exhibits a low level of toxicity to normal tissues when administered intravenously at concentrations below 400 mg/m^2 [13]. The detailed mechanism of LND action remains controversial. The initial claim that LND inhibited glycolysis at the level of mitochondrial hexokinase 2 [14] was based on decreases in extracellular L-lactic acid. However, it was subsequently shown that LND increased intracellular L-lactate and lowered the intracellular pH (pHi) and nucleoside triphosphate levels of human melanoma xenografts. It was proposed that these effects reflected inhibition of the transport of L-lactic acid across the plasma membrane mediated by the proton-linked monocarboxylate transporter (MCT) [15-17], but no direct evidence for this was provided. Nor was consideration given to which of the four MCT isoforms known to transport L-lactate [18] might be inhibited. Another MCT inhibitor, α-cyano-4'-hydroxycinnamate (CHC), has been shown to exert similar effects to LND [19], but CHC is known to be substantially more potent an inhibitor of the mitochondrial pyruvate carrier (MPC) [18;20]. This led Nath *et al.* [5;21] to suggest that LND might also inhibit the MPC, although once again no direct evidence was presented. There is also evidence that LND inhibits mitochondrial respiration with different affinities for different substrates, but the exact sites of inhibition remains to be determined [22].

In this paper, we directly determine the effects of LND on MPC and MCT activity and show that the drug inhibits both processes with $K_{0.5}$ values of 2.5 and 36-40 μM, respectively. We also investigate the effects of LND on uncoupled respiration of heart and liver mitochondria. In agreement with Floridi and Lehninger [22], we demonstrate that pyruvate oxidation is substantially more sensitive to inhibition by LND (IC_{50} ~7.5 μM) than that of glutamate plus malate (IC_{50} ~25 μM) or succinate (IC_{50} ~150 μM). We further demonstrate that in isolated DB-1 melanoma cells 1-10 μM LND increased L-lactate output, consistent with MPC inhibition, but at higher concentrations (150 μM) L-lactate output decreased while intracellular [L-lactate] increased > five-fold, consistent with MCT inhibition. Taken together, our data suggest that the combined inhibition of the MPC and MCTs by LND prevents both efflux of glycolytically derived L-lactic acid from the cell and its oxidation by mitochondria. The resulting decrease in intracellular pH inhibits glycolysis and, with the cell unable to compensate by oxidizing L-lactate / pyruvate, the cell experiences a bioenergetics crisis which is made worse by the effects of LND on the oxidation of other substrates such as glutamine. The combination of these effects can account for the increase in L-lactic acid and decrease in ATP levels as well as intracellular acidification that have been noted previously [4;5;15-17;21].

EXPERIMENTAL

Materials

Radiochemicals were purchased from PerkinElmer Life Sciences (Beaconsfield, Bucks.,U.K.) while all other chemicals and biochemicals were obtained from Sigma-Aldrich or Merck via VWR international Ltd (Poole, Dorset., U.K.).

Methods

Preparation of rat heart and liver mitochondria

Hearts and livers were taken from male Wister rats (~275 g) and mitochondria prepared as described previously [23] by Dounce-Potter homogenisation at 4°C in isolation buffer (ISB: 300 mM sucrose, 2 mM EGTA and 10 mM Tris/HCl, pH 7.1) supplemented with 5 mg / mL fatty acid free bovine serum albumin) followed by differential centrifugation, Percoll® density gradient centrifugation and washing in ISB without albumin. For heart mitochondria, the heart was finely chopped and incubated with bacterial protease prior to homogenisation as described elsewhere [24].

Oxygen electrode studies

Rat liver (1 mg protein) or heart mitochondria (0.5 mg protein) were added to 2 mL respiration buffer (125 mM KCl, 20 mM MOPS, 10 mM Tris, 2.5 mM KPi, 0.5 mM EGTA, pH 7.2) in the chamber of an oxygen electrode (Hansatech Oxygraph) that was maintained at 30^{o}C. The required substrates were then added (5 mM succinate plus 1 µM rotenone; 5 mM L-glutamate plus 2 mM L-malate or 1 mM pyruvate plus 0.5 mM L-malate) and rates of respiration determined before and after sequential additions of 0.5 mM ADP, uncoupler (0.1 µM carbonyl cyanide p-trifluoromethoxyphenylhydrazone – FCCP) and the required concentration of LND or CHC. Further details are given in the Figure legends.

Measurement of mitochondrial pyruvate transport

This was performed in a cold-room (4^{o}C) by measuring the uptake of [1-^{14}C] pyruvate into liver mitochondria at 9^{o}C using a modification of the dual label isotope technique described previously [20]. Uptake was terminated after 45 s (the linear phase of transport) by rapid sedimentation of mitochondria using a microcentrifuge. In outline, mitochondria were incubated on ice at 6 mg protein / mL in ISA containing the required concentration of LND. After 2 min, an aliquot (2 mL) was mixed with 3 mL of assay buffer (125 mM KCl, 20 mM MOPS, 0.5 mM EGTA, 1 µM rotenone at pH 6.8 and 20^{o}C) containing [1-^{14}C] pyruvate (0.1 mM and 5,000 Bq/mL) and $^{3}H_2O$ (25,000 Bq/mL) and then four 1 mL aliquots were immediately transferred to 1.5 mL microcentrifuge tubes. The tubes were transferred to an Eppendorff microcentrifuge (5415C) and, exactly 45 s after initial mixing, centrifuged at 10,000g for 1 min. The supernatants were rapidly removed and added to 0.1 mL 20% (w/v) perchloric acid (PCA) while the pellet was extracted in 0.5 mL water and 50 µL PCA (20% w/v) added. After removal of precipitated protein by centrifugation, samples of the pellet (0.5 mL) and supernatant (0.1 mL) were then assayed for [^{14}C] and [^{3}H] using a Packard TriCarb 2100 scintillation counter. A parallel experiment in which [U-^{14}C] sucrose replaced the [1-^{14}C] pyruvate was performed to enable the intra-mitochondrial [1-^{14}C] pyruvate to be calculated from the total [1-^{14}C] pyruvate in the pellet [20].

Measurement of the rate of L-lactate uptake by Xenopus oocytes expressing different MCT isoforms

This was carried out as described in detail elsewhere [25;26]. In outline, pGHJ plasmids containing the required MCT isoform were transcribed into cRNA which was then microinjected into *Xenopus laevis* oocytes. These were incubated for 3 days at 19°C to allow expression of the appropriate MCT at the plasma membrane of the oocyte. L-Lactate transport into individual oocytes was then measured by incubating at room temperature (22°C) in assay buffer (75 mM NaCl, 2 mM KCl, 0.82 mM $MgCl_2$, 1 mM $CaCl_2$, 20 mM MES, pH 6.0) containing [U-^{14}C] L-lactate (0.5 mM and 7.4 MBq / mL) and the required concentration of LND. Lactate uptake was confirmed to be linear with time for 5 min under these conditions [25;26]. Oocytes were then rapidly washed in ice-cold assay buffer prior to lysis in 0.5% (w/v) SDS and measurement of intracellular [U-^{14}C]-L-lactate by scintillation counting.

Cell culture and LND treatment

DB-1 human melanoma cells [27] were cultured in RPMI medium supplemented with 10% fetal bovine serum, 100 units/mL penicillin, and 100 mg/liter streptomycin. LND was freshly prepared in DMSO. DB-1 cells were treated for 1 h with vehicle (0.1% (v/v) DMSO) or LND (1, 10, 40 or 150 μM) in RPMI medium without phenol red and fetal bovine serum. Three individual plates of cells were used per treatment condition.

L-Lactate measurement

Intracellular and extracellular L-lactate was measured as previously described [28] with modification. DB-1 cells were washed twice with phosphate-buffered saline (PBS) followed by scraping into 750 μL of ice-cold methanol/water (4:1, v/v) containing 2.5 μg of [$^{13}C_3$] lactate as internal standard. Samples were pulse-sonicated for 30 s. Medium collected from cell culture was centrifuged at 1,000 x g for 5 min to remove floating cells. Medium supernatant (200 μL) was mixed with 800 μL of ice-cold methanol and 75 ng of [$^{13}C_4$] succinate as internal standard. Both sonicated cell lysates and medium were then centrifuged at 16,000 × *g* for 10 min. The supernatants were transferred to clean tubes and evaporated to dryness under nitrogen. The dried residues were re-suspended in 100 μL of water. L-lactate was analyzed using an Agilent 1200 series HPLC system coupled to an Agilent 6460 triple quadrupole mass spectrometer equipped with an electrospray ionization source operated in the negative ion mode. Analytes were separated by reversed-phase ion-pairing chromatography utilizing a Phenomenex Luna C_{18} column (150 × 2.00 mm, 3-μm particle size) at a flow rate of 200 μL/min maintained at 45°C. A two-solvent gradient system was used with solvent A as 200 mM 1,1,1,3,3,3-hexafluoro-2-propanol and 5 mM ethyldiisopropylamine (DIPEA) in water and solvent B as 200 mM 1,1,1,3,3,3-hexafluoro-2-propanol and 5 mM DIPEA in methanol. The linear gradient conditions were as follows: 2% B at 0 min, 2% B at 4 min, 95% B at 9 min, 95% B at 12.5 min, 2% B at 13 min followed by a 4-min equilibration.

Data fitting

For the calculation of $K_{0.5}$ values for LND inhibition of L-lactate and pyruvate transport, data were fitted by least squares regression analysis to the equation below using FigSys (Biosoft, Cambridge):

$$\text{Rate as \% control} = 100 / (1+ ([I]/K_{0.5})^n)$$

[I] is the concentration of LND and n, the Hill coefficient which was set to 1 for mitochondrial pyruvate transport where no evidence of cooperativity was observed, and thus K0.5 represents the dissociation constant (K_i) of the inhibitor from the MPC. The $K_{0.5}$ and n values determined from the fitted data are given ± the standard error (S.E.). For LND inhibition of respiration, data were fitted using the Bezier Spline function of FigSys except in the case of pyruvate oxidation by heart mitochondria. In this case data were fitted to an equation that assumes oxidation of pyruvate is set by the activity of PDH which in turn is controlled by the rate of pyruvate transport relative to that of PDH. The principle behind this approach and the mathematical analysis used is similar to that described previously [29]. In outline, the rate of pyruvate oxidation (V) is expressed in terms of the intramitochondrial [pyruvate] (P_{in}) assuming Michaelis Menten kinetics:

$$v = V_{pdh} \times [P_{in}]/(P_{in} + K_{pdh}) \qquad \textit{Equation 1}$$

where V_{pdh} is the V_{max} of PDH expressed as % of the rate of pyruvate oxidation in the absence of LND, and K_{pdh} is the K_m of PDH (set at 40 μM [30]). This rate of pyruvate oxidation must also be the same as the net rate of pyruvate transport expressed as the influx rate minus the efflux rate. This is given by:

$$v = (V_{mpc} \times [P_{out}]/(P_{out} + K_{mpc}) - V_{mpc} \times [P_{in}]/(P_{in} + K_{mpc})) \times A \qquad \textit{Equation 2}$$

where V_{mpc} is the V_{max} of the MPC expressed as % of the rate of pyruvate oxidation in the absence of LND, K_{mpc} is the K_m of MPC (set at 150 μM [20]), $[P_{out}]$ the extramitochondrial [pyruvate], and A the activity of the MPC in the presence of LND expressed as a fraction of the activity in the absence of LND. The value of A is itself calculated assuming that LND inhibits competitively with pyruvate on the inner face of the MPC as is the case for CHC [31] and that the concentration of LND in the matrix is the same as in the medium. Thus:

$$A = (P_{in} + K_{mpc})/(P_{in} + K_{mpc} \times (1+I/K_i)) \qquad \textit{Equation 3}$$

where I is the concentration of LND and K_i its dissociation constant. Combining equations 1 and 2 generates a quadratic equation from which $[P_{in}]$ can be calculated using regression analysis and hence the rate of pyruvate oxidation using Equation 1. It should be noted that for simplicity our analysis has ignored any small MPC-independent rate of pyruvate transport into mitochondria. We have reanalyzed the data including such a parameter but the calculated value for the inhibitor independent rate was not significantly different from zero. For all analyses using regression analysis, the parameter values are derived with standard errors (S.E.) and thus a 95% confidence interval (2 × S.E). Values were only considered significantly different when there was no overlap in this value.

RESULTS

LND inhibits mitochondrial pyruvate transport with a K_i of 2.5 μM

We used isolated rat liver mitochondria to investigate whether LND inhibits the mitochondrial pyruvate carrier (MPC). Uptake of [1-^{14}C] pyruvate (60 μM) was measured

at 45 s in the presence of rotenone and 9°C to prevent significant pyruvate metabolism. To ensure accumulation of pyruvate, uptake was energised using an artificially induced pH gradient (pH 6.8 outside, pH 7.4 inside) as described under Methods. We have previously validated this method as suitable to provide true initial rates of pyruvate transport [20]. As shown in Fig. 1A, increasing concentrations of LND produced a progressive inhibition of pyruvate uptake with a K_i value (± S.E. of the fit shown) of 2.5 ± 0.1 μM. Fig. 1A also includes data for inhibition of the mitochondrial pyruvate carrier by the well-characterised MPC inhibitor, CHC, which produced >90% inhibition at 10 μM. We confirmed the inhibition of mitochondrial pyruvate transport in rat heart mitochondria by measuring the effects of LND on the rate of uncoupled pyruvate-dependent respiration at 30°C as shown in Fig. 1B. The lowest concentration of LND used (2 μM) was without effect on pyruvate oxidation since the MPC does not limit respiration under these conditions [32]. However, after addition of 3 μM LND, significant (~15%) inhibition was observed and approached 70% by 10 μM, close to the inhibition of pyruvate transport in liver mitochondria by 10 μM CHC. As described in Methods, we were able to fit the data to an equation that assumes oxidation of pyruvate is set by the activity of PDH which in turn is controlled by the rate of pyruvate transport relative to that of PDH. The fit shown in Fig. 1B assumes published K_m values for the MPC (150 μM) and PDH (40 μM) and the K_i for LND of 2.5 μM derived from the data of Fig. 1A. The calculated V_{max} values for PDH and the MPC (± S.E. and expressed as a percentage of the maximum rate of oxygen consumption in the absence of LND) were 127 ± 6.3 and 233 ± 9.1, respectively. This analysis confirms that the IC_{50} for LND inhibition of uncoupled pyruvate oxidation (~ 7.5 μM) is entirely consistent with its inhibition of the MPC whose activity is significantly greater than that of PDH.

LND cooperatively inhibits MCT1, MCT2 and MCT4 less potently than MPC

The effects of LND on L-lactate transport by MCT1, MCT2 and MCT4 were investigated using *Xenopus laevis* oocytes expressing each of the isoforms individually. This was achieved by microinjection of the relevant cRNA and culture for 72 hr as described previously [25]. In the case of MCT2, co-injection of the cRNA for embigin, the preferred ancillary protein of MCT2 [33], was required to give high expression levels of the transporter, whereas for MCT1 and MCT4 maximal levels of expression were supported by endogenous basigin [25;26]. Expression of each of the MCT isoforms gave a similar enhancement of 0.5 mM [U-^{14}C] L-lactate transport compared to water-injected oocytes as shown in Fig.2A. Increasing concentrations of LND produced a progressive inhibition of L-lactate uptake for all isoforms as shown in Panels B-D of Fig. 2. Data are expressed as percentage of rates in the absence of inhibitor to allow easier comparison between experiments on different days and with different isoforms. For each isoform, data could be fitted using the equation for cooperative non-competitive inhibition as described under Methods. Derived $K_{0.5}$ values (± S.E. of the fit shown) for MCT1, MCT2 and MCT4 are 36.8 ± 3.1, 36.4 ± 3.6 and 40.4 ± 2.2 μM, respectively, with corresponding values for the Hill coefficient of 1.65 ± 0.23, 1.86 ± 0.34 and 1.84 ± 0.19.

LND inhibits uncoupled mitochondrial pyruvate oxidation more potently than glutamate + malate or succinate oxidation.

Previous reports have suggested that LND affects mitochondrial respiration with different sensitivities depending on the substrate employed (Floridi & Lehninger, 1983). Figure 3A shows that the effect of LND on uncoupled pyruvate oxidation by rat heart mitochondria was significantly greater than that on the oxidation of other respiratory substrates, which is entirely consistent with a dominant effect of the inhibitor on the MPC as opposed to the respiratory chain. Liver mitochondria, unlike heart mitochondria, do not oxidize pyruvate rapidly, and the MPC does not exert much control over its oxidation [34]. However, uncoupled respiration in the presence of either glutamate + malate or succinate (in the presence of rotenone) is rapid and the data of Fig. 3B confirm that LND inhibits both with IC_{50} values of 25 and 150 μM, respectively. The data with succinate closely match similar data obtained in uncoupled mouse liver mitochondria where we also demonstrated that LND inhibits succinate-ubiquinone reductase activity of respiratory complex II with an IC_{50} of about 300 μM [28]. This is substantially higher than the K_i for the MPC and IC_{50} for pyruvate and glutamate + malate oxidation. It should be noted that for both liver and heart mitochondria the inhibition of glutamate + malate oxidation by LND appears to be biphasic. We have not investigated this further, but it could reflect two pathways of glutamate oxidation known to operate in isolated mitochondria. Oxidation via glutamate dehydrogenase can occur, especially in liver mitochondria. However, the more prominent pathway is via transamination with oxaloacetate, formed by malate oxidation, to yield aspartate, which leaves the mitochondria in exchange for the incoming glutamate on the glutamate / aspartate carrier [35;36].

Effects of LND on L-lactate output by DB-1 melanoma cells

It would be predicted that inhibition of the MPC by low concentrations of LND (MPC specific) would cause a decrease in pyruvate oxidation and thus an increase in L-lactate output as glycolysis compensates for the resulting decrease in mitochondrial ATP production. Conversely, higher LND concentrations, which also inhibit the MCTs, should decrease L-lactic acid efflux with a corresponding rise in intracellular [L-lactate]. We performed experiments with isolated DB-1 melanoma cells that confirmed this prediction as shown in Fig. 4. We found that 1-10 μM LND increased L-lactate output (Panel A), consistent with MPC inhibition, and this occurred without a detectable increase in intracellular [L-lactate] (Panel B). However, higher LND concentrations, 40 μM and 150 μM, caused intracellular [L-lactate] to increase by two-fold and eight-fold, respectively, (Panel B) with a corresponding decrease in L-lactate output, consistent with MCT inhibition (Panel A).

DISCUSSION

Mitochondrial sites of action of lonidamine on tumour cell energy metabolism

In 1981, Floridi *et al.* reported that in Ehrlich ascites and various other tumour cells LND inhibited respiration as well as aerobic and anaerobic glycolysis, but had no effect on normal rat Sertoli cells [14;37;38]. They attributed the selective inhibition of glycolysis in tumour cells by LND to its inhibition of mitochondria-bound hexokinase 2 that Pedersen *et al.* [39] had shown was strongly expressed in many tumour cells. However, subsequent studies demonstrated that LND directly inhibited the uncoupled respiration of mitochondria from Ehrlich ascites fueled by various NAD- and FAD-linked substrates but not duroquinol, that feeds electrons directly into complex 3, or ascorbate + N,N,N',N'-tetramethyl-*p*-phenylenediamine (TMPD) that feeds electrons into complex 4 via cytochrome *c* [22;40]. The authors concluded that LND inhibits succinate oxidation within complex 2 of the respiratory chain, which our subsequent studies confirmed [28], while oxidation of pyruvate + malate and other NAD-linked substrates involved a decrease in mitochondrial NADH generation, which might indicate inhibition of dehydrogenases activity. The data we present in Fig. 1B and Fig. 3 are entirely consistent with this proposal but suggest that the more potent effect on pyruvate oxidation actually reflects the inhibition of the MPC by LND.

Lonidamine is a potent inhibitor of the mitochondrial pyruvate carrier

In Fig. 1A, we demonstrate directly that LND inhibits the MPC with a K_i of 2.5 ± 0.1 μM, which is similar to the K_i value determined previously for the well-established MPC-inhibitor CHC [20]. Fig. 1B confirms that this inhibition can account for the inhibition profile of uncoupled oxidation of pyruvate by isolated heart mitochondria. These data were fitted to an equation that assumes oxidation of pyruvate is set by the activity PDH which in turn is controlled by the rate of pyruvate transport relative to that of PDH. Using the derived K_i value for LND of 2.5 μM, the data generated V_{max} values for PDH and the MPC (± S.E. and expressed as a percentage of the maximum rate of oxygen consumption in the absence of LND) of 127 ± 6.3 and 233 ± 9.1, respectively. Since the rate of oxygen consumption in the absence of LND is known (87.9 ± 5.8 nmol O_2 . min^{-1} per mg protein), the V_{max} values for PDH and the MPC can be calculated as 112 and 205 nmol O_2 . min^{-1} per mg protein, respectively. If it is assumed that pyruvate is oxidized totally to CO_2 and water, then 2.5 nmol O_2 are used to oxidize 1 nmol of pyruvate, and this allows calculation of true V_{max} values for PDH and the MPC at 30°C of 45 and 82 $nmol.min^{-1}$ per mg protein. By measuring the temperature-dependence of the proton fluxes associated with mitochondrial pyruvate uptake, the activation energy of the MPC in rat liver mitochondria was determined to be 113 $kJ.mol^{-1}$ [20]. Using this value, together with the K_m of the MPC (150 μM [20]) and the rate of transport measured directly at 9°C and 60 μM pyruvate in Fig. 1A (0.303 nmol per mg protein in 45s), the V_{max} of the MPC in liver mitochondria at 30°C can be calculated to be 34.7 $nmol.min^{-1}$ per mg protein. The concentrations of the MPC in rat heart and liver mitochondria were determined by inhibitor binding studies to be 56 and 26 pmol per mg protein, respectively [32], and this would give a value for the V_{max} of the MPC in heart mitochondria of 74.8 $nmol.min^{-1}$ per mg protein, which is in reasonable agreement with the value of 82 $nmol.min^{-1}$ per mg protein derived from the data of Fig. 1B.

Lonidamine also inhibits MCT1, MCT2 and MCT4, but less potently than the MPC. There are four members of the proton-linked monocarboxylate transporter (MCT) family that are known to transport L-lactate of which the dominant isoforms expressed in tumour cells are MCT1 and MCT4 with some tumours also expressing MCT2 [18;41]. The data of Fig. 1 show that each of these isoforms is inhibited cooperatively by LND with similar values for $K_{0.5}$ and Hill coefficients of 36-40 μM and 1.65-1.85, respectively. The $K_{0.5}$ value is more than an order of magnitude higher than its K_i for inhibition of the MPC, a characteristic also displayed by CHC [18]. However, the ability of LND to inhibit L-lactate transport by all three MCT isoforms with a similar potency is quite different from other well-established MCT inhibitors such as CHC and 6-[(3,5-Dimethyl-1H-pyrazol-4-yl)methyl]-5-[[(4S)-4-hydroxy-2-isoxazolidinyl]carbonyl]-3-methyl-1-(2-methylpropyl)thieno[2,3-d]pyrimidine-2,4(1H,3H)-dione (AR-C155858). These inhibitors bind to the substrate binding site of the transporter and like substrates show a much higher affinity for MCT1 and MCT2 than MCT4 [25;42;43]. It may also be significant that inhibition by LND, unlike CHC and AR-C155858, is cooperative with a Hill coefficient that is close to 2. MCTs operate as dimers in association with two copies of the ancillary protein embigin or basigin [44], and thus it is possible that LND binds at an interface of the two MCT monomers that are shared by all isoforms.

Integrating the known actions of lonidamine into a mechanism for its anti-tumour effects

Carbon-13 NMR studies of perfused DB-1 melanoma cells indicate that these tumours obtain about 46% of their ATP from glycolysis and 54% from oxidative phosphorylation [45]. Under *in vivo* conditions, substantial levels of hypoxia would be anticipated, increasing the glycolytic contribution; but given its much higher ATP-production efficiency, oxidative metabolism would still account for a large fraction of tumour energy production. Our data indicate that the most avid target site for LND is the MPC (K_i, 2.5 μM) while half maximal inhibition of the MCT1 and MCT4 (the two MCT isoforms expressed in DB-1 cells [46]) only occurs at 36-40 μM, more than an order of magnitude greater. The inhibition of the MPC by LND accounts for its ability to inhibit pyruvate oxidation with an IC_{50} of ~7.5 μM which is substantially lower than its IC_{50} for inhibition of other respiratory substrates (25 μM for glutamate plus malate and 150 μM for succinate). Thus, it would be predicted that the lowest concentrations of LND will only inhibit pyruvate oxidation leading to increase rates of glycolysis and L-lactic acid production. The data of Fig. 4A confirm this prediction in DB-1 melanoma cells. At higher LND concentrations, oxidation of glutamine (via glutamate) would also be inhibited which has the potential to enhance glycolysis further. However we do not observe a further increase in L-lactate output, probably because these higher LND concentrations will also begin to inhibit L-lactic acid efflux on MCT1 and MCT4. The data of Fig. 4B confirm this since intracellular [L-lactate] increases by two-fold and eight-fold at 40 μM and 150 μM LND, respectively. MCT1 and MCT4 are expressed about equally in DB-1 melanoma cells [46], and although both are inhibited with a similar $K_{0.5}$, the effect on MCT4 is likely to be less significant initially since MCT1 has a much lower K_m (5 mM) than MCT4 (25

mM) [18] and thus will be responsible for the majority of L-lactic acid efflux at the lower intracellular [L-lactate].

As inhibition of MCT1 and MCT4 increases at higher [LND], the accumulation of intracellular L-lactate would be predicted to cause a drop in pHi. Our previous studies using DB-1 xenografts in mice that were injected with LND (100 mg/kg, i.p.) detected such changes [5]. Thus, using P-31 NMR to measure pHi and energy status, and H-1 NMR to measure intracellular [L-lactate], we demonstrated a selective decrease in tumour pHi from 6.9 ± 0.1 to 6.3 ± 0.1 within about 40 min of LND treatment. This was associated with a three-fold rise in [L-lactate]. No significant change in pHi of normal muscle or brain was detected, and only a slight transient change in pHi of liver was observed at 20 min post-injection [5]. A slight decrease in extracellular pH of the tumour (~0.2 pH units) was also observed and could be explained by some of the increased L-lactic acid produced leaving the cell via residual MCT activity and via free diffusion which is enhanced at low pH [18]. Concomitant with these changes, there was a slow monotonic decrease in the bioenergetic status of the tumour consisting of a decrease in nucleoside triphosphates (including ATP) and an increase in inorganic phosphate (Pi). The overall effect was a 66.8 ± 5.7% decrease in the NTP/Pi ratio within about 3 hr [5]. Again this bioenergetic decline is tumour specific, with no change in the NTP/Pi ratio of muscle and brain and only a transient small decrease in NTP/Pi of the liver at 40 min post-injection of the drug.

It would seem likely that the ability of LND to inhibit the MPC is critical because it may enhance the consequences of inhibiting MCT activity by preventing oxidation of the accumulated L-lactate through its conversion to pyruvate, entry into the mitochondria and oxidation via PDH and the citric acid cycle. This prevents the cell from compensating for the loss in glycolytic ATP by up-regulating oxidative phosphorylation, an effect further curtailed by inhibition of the respiratory chain. Recently, the effects on cancer cell growth and metabolism on knocking down Mpc1 and Mpc2, two proteins recently identified as components of the MPC [47;48], have been investigated [49;50]. Mpc1 was shown to be down-regulated or absent in many tumours and its over-expression impaired tumour cell growth [49], which does not fit easily with our data implicating inhibition of the MPC in the anti-tumour effects of LND. However, although it is now widely accepted that Mpc1 and Mpc2 form a multimeric MPC complex [51], questions have been raised over whether these proteins might exert their effects on pyruvate metabolism rather than transport [52]. In this context, it may be significant that measurement of the isotope flux of [^{13}C] into citrate from [U-^{13}C]-glucose and [U-^{13}C]-glutamine shows the specific MPC inhibitor UK5099 to have a much more profound effect on the labelling pattern of citrate than does Mpc1 or Mpc2 knockdown [50].

Conclusions

Our data suggest that the combined inhibition of the MPC and MCTs by LND prevents both efflux of glycolytically derived L-lactic acid from the cell and its oxidation by mitochondria. The resulting decrease in intracellular pH inhibits glycolysis and with the cell unable to compensate by oxidizing L-lactate / pyruvate, the cell experiences a bioenergetic crisis which is aggravated by the effects of LND on the oxidation of other

substrates such as glutamine. This proposal is supported by published data on the selective tumour effects of LND on L-lactate, pHi and ATP levels [5] and by similar effects described for the established MPC and MCT inhibitor α-cyano-4-hydroxycinnamate [19]. Delineation of why LND appears to be tumour-specific when all cells are dependent on the activity of either or both the MPC and MCTs remains to be determined. However, it could simply reflect the expression levels of MCT isoforms and the MPC relative to rates of metabolism dependent on them.

Acknowledgements We thank Lovemore Kuzumunhu for assistance with preliminary experiments on mouse liver mitochondria and Stephen Tuttle and Cameron Koch for useful discussions and sharing of resources.

Declaration of Interests None

Funding Information This research was performed with support from NIH grants R01-CA129544 and R01-CA172820 (both JDG).

Author Contributions. BN and APH performed the experiments providing the data for Figs 1-3 at Bristol University. Parallel studies of respiration of mouse liver mitochondria were performed at UPenn by LG, RZ, KN and DSN with guidance from APH. LND treatment of DB-1 cells and lactate measurement (Fig. 4) were performed at UPenn by LG and DSN using facilities in laboratories of JDG and IAB. Overall planning and design of the experiment was conducted by APH, JDG, IAB and DBL. Preparation and editing of the manuscript was performed by APH, JDG, DSN and DBL. Funding for the project was secured by JDG with assistance from KN, DSN, IAB and DBL.

REFERENCES

1 Cioli, V., Bellocci, B., Putzolu, S., Malorni, W. and Demartino, C. (1980) Anti-spermogenic activity of Lonidamine (AF-1890) in rabbit. Ultramicroscopy **5**, 418-418

2 Band, P. R., Maroun, J., Pritchard, K., Stewart, D., Coppin, C. M., Wilson, K. and Eisenhauer, E. A. (1986) Phase II study of lonidamine in patients with metastatic breast cancer: a National Cancer Institute of Canada Clinical Trials Group Study. Cancer Treat. Rep. **70**, 1305-1310

3 Weinerman, B. H., Eisenhauer, E. A., Besner, J. G., Coppin, C. M., Stewart, D. and Band, P. R. (1986) Phase II study of lonidamine in patients with metastatic renal cell carcinoma: a National Cancer Institute of Canada Clinical Trials Group Study. Cancer Treat. Rep. **70**, 751-754

4 Nath, K., Nelson, D. S., Heitjan, D. F., Zhou, R., Leeper, D. B. and Glickson, J. D. (2015) Effects of hyperglycemia on lonidamine-induced acidification and de-energization of human melanoma xenografts and sensitization to melphalan. NMR Biomed. **28**, 395-403

5 Nath, K., Nelson, D. S., Ho, A. M., Lee, S. C., Darpolor, M. M., Pickup, S., Zhou, R., Heitjan, D. F., Leeper, D. B. and Glickson, J. D. (2013) (31) P and (1) H MRS of DB-1 melanoma xenografts: lonidamine selectively decreases tumor intracellular pH and energy status and sensitizes tumors to melphalan. NMR Biomed. **26**, 98-105

6 Floridi, A., Gambacurta, A., Bagnato, A., Bianchi, C., Paggi, M. G., Silvestrini, B. and Caputo, A. (1988) Modulation of adriamycin uptake by lonidamine in Ehrlich ascites tumor cells. Exp. Mol. Pathol. **49**, 421-431

7 Prabhakara, S. and Kalia, V. K. (2008) Optimizing radiotherapy of brain tumours by a combination of temozolomide & lonidamine. Indian J. Med. Res. **128**, 140-148

8 Silvestrini, B., Hahn, G. M., Cioli, V. and De Martino, C. (1983) Effects of lonidamine alone or combined with hyperthermia in some experimental cell and tumour systems. Br. J. Cancer **47**, 221-231

9 Ning, S. C. and Hahn, G. M. (1991) Combination therapy: lonidamine, hyperthermia, and chemotherapy against the RIF-1 tumor in vivo. Cancer Res. **51**, 5910-5914

10 Kim, J. H., Alfieri, A. A., Kim, S. H. and Young, C. W. (1986) Potentiation of radiation effects on two murine tumors by lonidamine. Cancer Res. **46**, 1120-1123

11 Kim, J. H., Alfieri, A., Kim, S. H., Young, C. W. and Silvestrini, B. (1984) Radiosensitization of Meth-A fibrosarcoma in mice by Lonidamine. Oncology **41 Suppl 1**, 36-38

12 Golding, J. P., Wardhaugh, T., Patrick, L., Turner, M., Phillips, J. B., Bruce, J. I. and Kimani, S. G. (2013) Targeting tumour energy metabolism potentiates the cytotoxicity of 5-aminolevulinic acid photodynamic therapy. Br. J. Cancer **109**, 976-982

13 Price, G. S., Page, R. L., Riviere, J. E., Cline, J. M. and Thrall, D. E. (1996) Pharmacokinetics and toxicity of oral and intravenous lonidamine in dogs. Cancer Chemother. Pharmacol. **38**, 129-135

14 Floridi, A., Paggi, M. G., D'Atri, S., De Martino, C., Marcante, M. L., Silvestrini, B. and Caputo, A. (1981) Effect of lonidamine on the energy metabolism of Ehrlich ascites tumor cells. Cancer Res. **41**, 4661-4666

15 Mardor, Y., Kaplan, O., Sterin, M., Ruiz-Cabello, J., Ash, E., Roth, Y., Ringel, I. and Cohen, J. S. (2000) Noninvasive real-time monitoring of intracellular cancer cell metabolism and response to lonidamine treatment using diffusion weighted proton magnetic resonance spectroscopy. Cancer Res. **60**, 5179-5186

16 Ben-Yoseph, O., Lyons, J. C., Song, C. W. and Ross, B. D. (1998) Mechanism of action of lonidamine in the 9L brain tumor model involves inhibition of lactate efflux and intracellular acidification. J. Neurooncol. **36**, 149-157

17 Ben-Horin, H., Tassini, M., Vivi, A., Navon, G. and Kaplan, O. (1995) Mechanism of action of the antineoplastic drug lonidamine: 31P and 13C nuclear magnetic resonance studies. Cancer Res. **55**, 2814-2821

18 Halestrap, A. P. (2013) Monocarboxylic acid transport. Compr. Physiol. **3**, 1611-1643

19 Zhou, R., Bansal, N., Leeper, D. B., Pickup, S. and Glickson, J. D. (2001) Enhancement of hyperglycemia-induced acidification of human melanoma xenografts with inhibitors of respiration and ion transport. Acad. Radiol. **8**, 571-582

20 Halestrap, A. P. (1975) The mitochondrial pyruvate carrier - Kinetics and specificity for substrates and inhibitors. Biochem. J. **148**, 85-96

21 Nath, K., Nelson, D. S., Heitjan, D. F., Leeper, D. B., Zhou, R. and Glickson, J. D. (2015) Lonidamine induces intracellular tumor acidification and ATP depletion in breast, prostate and ovarian cancer xenografts and potentiates response to doxorubicin. NMR Biomed. **28**, 281-290

22 Floridi, A. and Lehninger, A. L. (1983) Action of the antitumor and antispermatogenic agent lonidamine on electron transport in Ehrlich ascites tumor mitochondria. Arch. Biochem. Biophys. **226**, 73-83

23 Davidson, A. M. and Halestrap, A. P. (1990) Partial Inhibition by Cyclosporin A of the swelling of liver mitochondria in vivo andin vitro induced by sub-micromolar [Ca2+] but not by butyrate Evidence for two distinct swelling mechanisms. Biochem. J. **268**, 147-152

24 Pasdois, P., Parker, J. E., Griffiths, E. J. and Halestrap, A. P. (2011) The role of oxidized cytochrome c in regulating mitochondrial reactive oxygen species production and its perturbation in ischaemia. Biochem. J. **436**, 493-505

25 Ovens, M. J., Davies, A. J., Wilson, M. C., Murray, C. M. and Halestrap, A. P. (2010) AR-C155858 is a potent inhibitor of monocarboxylate transporters MCT1 and MCT2 that binds to an intracellular site involving transmembrane helices 7-10. Biochem. J. **425**, 523-530

26 Ovens, M. J., Manoharan, C., Wilson, M. C., Murray, C. M., and Halestrap, A. P. (2010) Biochem. J. **431**, 217-225

27 Hill, L. L., Korngold, R., Jaworsky, C., Murphy, G., McCue, P. and Berd, D. (1991) Growth and metastasis of fresh human melanoma tissue in mice with severe combined immunodeficiency. Cancer Res. **51**, 4937-4941

28 Guo, L., Shestov, A. A., Worth, A. J., Nath, K., Nelson, D. S., Leeper, D. B., Glickson, J. D. and Blair, I. A. (2016) Inhibition of Mitochondrial Complex II by the Anticancer Agent Lonidamine. J. Biol. Chem. **291**, 42-57

29 Thomas, A. P. and Halestrap, A. P. (1981) The role of mitochondrial pyruvate transport in the stimulation by glucagon and phenylephrine of gluconeogenesis from L-lactate in isolated rat hepatocytes. Biochem. J. **198**, 551-564

30 Tsai, C. S., Burgett, M. W. and Reed, L. J. (1973) Alpha-keto acid dehydrogenase complexes. XX. A kinetic study of the pyruvate dehydrogenase complex from bovine kidney. J. Biol. Chem. **248**, 8348-8352

31 Halestrap, A. P. (1978) Pyruvate and ketone-body transport across the mitochondrial membrane: exchange properties, pH-dependence and mechanism of

the carrier..Biochem. J. **172**, 377-387

32 Hildyard, J. C. W., Ammala, C., Dukes, I. D., Thomson, S. A. and Halestrap, A. P. (2005) Identification and characterisation of a new class of highly specific and potent inhibitors of the mitochondrial pyruvate carrier. Biochim. Biophys. Acta **1707**, 221-230

33 Wilson, M. C., Meredith, D., Fox, J. E. M., Manoharan, C., Davies, A. J. and Halestrap, A. P. (2005) Basigin (CD147) is the target for organomercurial inhibition of monocarboxylate transporter isoforms 1 and 4 - The ancillary protein for the insensitive MCT2 is embigin (Gp70). J. Biol. Chem. **280**, 27213-27221

34 Shearman, M. S. and Halestrap, A. P. (1984) The concentration of the mitochondrial pyruvate carrier in rat liver and heart mitochondria determined with α-cyano-β-(1-phenylindol-3-yl)acrylate. Biochem. J. **223**, 673-676

35 Borst, P. (1962) The pathway of glutamate oxidation by mitochondria isolated from different tissues. Biochim. Biophys. Acta **57**, 256-269

36 De Haan, E. J., Tager, J. M. and Slater, E. C. (1967) Factors affecting the pathway of glutamate oxidation in rat-liver mitochondria **131**, 1-13. Biochim. Biophys. Acta **131**, 1-13

37 Floridi, A., Paggi, M. G., Marcante, M. L., Silvestrini, B., Caputo, A. and De Martino, C. (1981) Lonidamine, a selective inhibitor of aerobic glycolysis of murine tumor cells. J. Natl. Cancer Inst. **66**, 497-499

38 Floridi, A., DeMartino, C., Marcante, M. L., Apollonj, C., Scorza Barcellona, P. and Silvestrini, B. (1981) Morphological and biochemical modifications of rat germ cell mitochondria induced by new antispermatogenic compounds: studies in vivo and in vitro. Exp. Mol. Pathol. **35**, 314-331

39 Mathupala, S. P., Ko, Y. H. and Pedersen, P. L. (2009) Hexokinase-2 bound to mitochondria: cancer's stygian link to the "Warburg Effect" and a pivotal target for effective therapy. Semin. Cancer Biol. **19**, 17-24

40 Floridi, A., Marcante, M. L., D'Atri, S., Feriozzi, R., Menichini, R., Citro, G., Cioli, V. and De Martino, C. (1983) Energy metabolism of normal and lonidamine-treated Sertoli cells of rats. Exp. Mol. Pathol. **38**, 137-147

41 Baltazar, F., Pinheiro, C., Morais-Santos, F., Azevedo-Silva, J., Queiros, O., Preto, A. and Casal, M. (2014) Monocarboxylate transporters as targets and mediators in cancer therapy response. Histol. Histopathol. **29**, 1511-1524

42 Manning Fox, J. E., Meredith, D. and Halestrap, A. P. (2000) Characterisation of human monocarboxylate transporter 4 substantiates its role in lactic acid efflux from skeletal muscle. J. Physiol. **529**, 285-293

43 Nancolas, B., Sessions, R. B. and Halestrap, A. P. (2015) Identification of key binding site residues of MCT1 for AR-C155858 reveals the molecular basis of its isoform selectivity. Biochem. J. **466**, 177-188

44 Wilson, M. C., Meredith, D. and Halestrap, A. P. (2002) Fluorescence resonance energy transfer studies on the interaction between the lactate transporter MCT1

and CD147 provide information on the topology and stoichiometry of the complex in situ. J. Biol. Chem. **277**, 3666-3672

45 Shestov, A. A., Mancuso, A., Leeper, D. B. and Glickson, J. D. (2013) Metabolic network analysis of DB1 melanoma cells: how much energy is derived from aerobic glycolysis? Adv. Exp. Med. Biol. **765**, 265-271

46 Wahl, M. L., Owen, J. A., Burd, R., Herlands, R. A., Nogami, S. S., Rodeck, U., Berd, D., Leeper, D. B. and Owen, C. S. (2002) Regulation of intracellular pH in human melanoma: potential therapeutic implications. Mol Cancer Ther. **1**, 617-628

47 Bricker, D. K., Taylor, E. B., Schell, J. C., Orsak, T., Boutron, A., Chen, Y. C., Cox, J. E., Cardon, C. M., Van Vranken, J. G., Dephoure, N., Redin, C., Boudina, S., Gygi, S. P., Brivet, M., Thummel, C. S. and Rutter, J. (2012) A mitochondrial pyruvate carrier required for pyruvate uptake in yeast, Drosophila, and humans. Science **337**, 96-100

48 Herzig, S., Raemy, E., Montessuit, S., Veuthey, J. L., Zamboni, N., Westermann, B., Kunji, E. R. and Martinou, J. C. (2012) Identification and functional expression of the mitochondrial pyruvate carrier. Science **337**, 93-96

49 Schell, J. C., Olson, K. A., Jiang, L., Hawkins, A. J., Van Vranken, J. G., Xie, J., Egnatchik, R. A., Earl, E. G., DeBerardinis, R. J. and Rutter, J. (2014) A role for the mitochondrial pyruvate carrier as a repressor of the Warburg effect and colon cancer cell growth. Mol. Cell **56**, 400-413

50 Yang, C., Ko, B., Hensley, C. T., Jiang, L., Wasti, A. T., Kim, J., Sudderth, J., Calvaruso, M. A., Lumata, L., Mitsche, M., Rutter, J., Merritt, M. E. and DeBerardinis, R. J. (2014) Glutamine oxidation maintains the TCA cycle and cell survival during impaired mitochondrial pyruvate transport. Mol. Cell **56**, 414-424

51 McCommis, K. S. and Finck, B. N. (2015) Biochem. J. **466**, 443-454

52 Halestrap, A. P. (2012) The mitochondrial pyruvate carrier: has it been unearthed at last? Cell Metab. **16**, 141-143

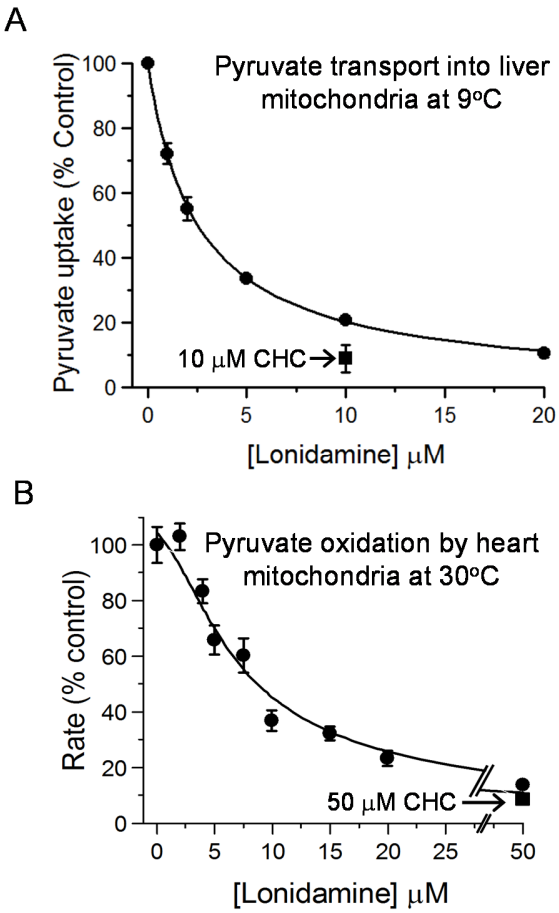

Figure 1 Lonidamine inhibits pyruvate transport into mitochondria
In Panel **A** pyruvate transport into liver mitochondria was assayed directly at 9°C using [1-^{14}C]-pyruvate as described under Methods. Data are presented as Means ± S.E.M. for 3 separate mitochondrial preparations. In each experiment, four replicates were performed at each LND concentration and the average value taken to calculate the extent of inhibition as percentage of control (no LND). Data were fitted to the standard inhibition equation (see Methods) to give a derived K_i value of 2.5 ± 0.1 μM. The absolute rate of pyruvate (60 μM) uptake in the absence of LND was 0.303 ± 0.032 nmol per mg protein in 45s. Panel **B** shows data for the inhibition of uncoupled pyruvate oxidation by isolated rat heart mitochondria at 30°C measured using an oxygen electrode as described under Methods. Mean data (± S.E.M.) are presented for 3 separate mitochondrial preparations. The absolute rate of pyruvate oxidation in the absence of LND was 87.9 ± 5.8 nmol O_2 . min^{-1} per mg protein. The data were fitted to an equation that assumes oxidation of pyruvate is set by the activity PDH which in turn is controlled by the rate of pyruvate transport relative to that of PDH as described under Methods. The K_i value for LND of 2.5 μM derived from Panel **A** was employed and the V_{max} of PDH and MPC activity (expressed as % control rate of oxygen consumption and ± S.E.) were then calculated by least squares regression analysis to be 127 ± 6.3 and 233 ± 9.1, respectively

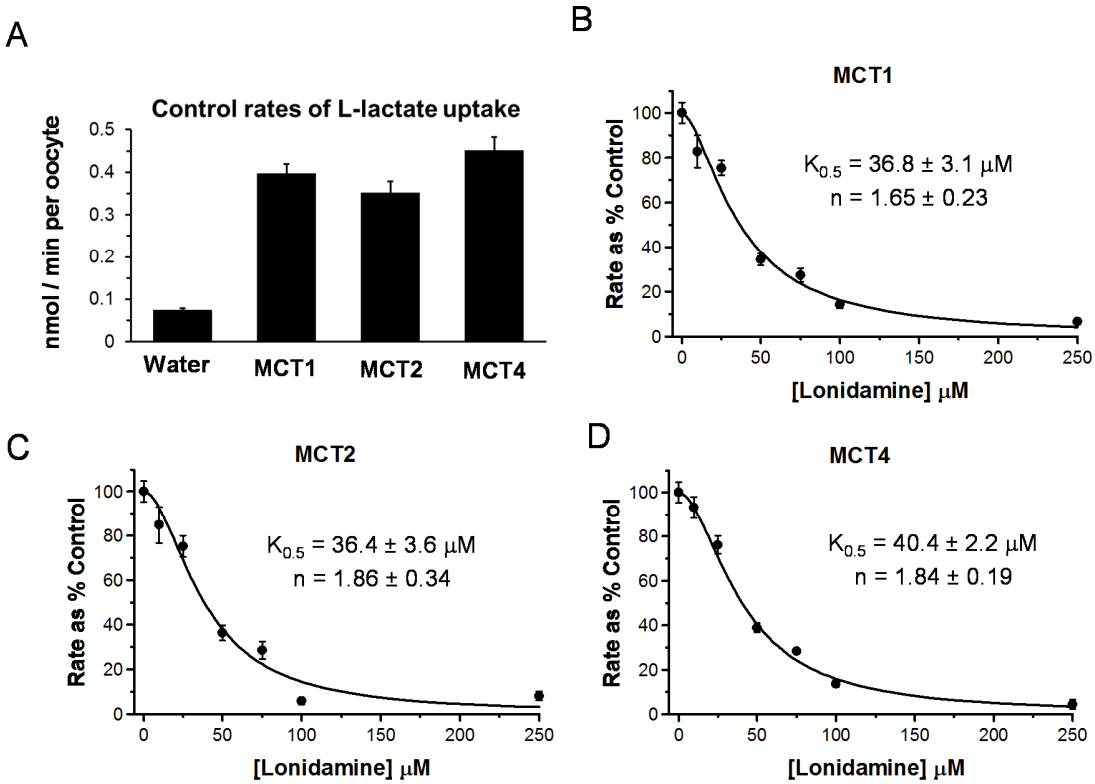

Figure 2 Lonidamine inhibits the proton-linked monocarboxylate carriers MCT1, MCT2 and MCT4

[U-^{14}C]-L-lactate uptake into *Xenopus laevis* oocytes expressing the MCT isoform indicated was determined as described in Methods. Panel **A** shows the absolute rates of L-lactate uptake while Panels **B-D** show the effects of increasing concentrations of LND on rates of L-lactate uptake into oocytes expressing MCT1, MCT2 or MCT4 as indicated. Rates are expressed as a percentage of the control (no LND) after subtraction of the uptake by water-injected oocytes. Each data point represents mean data ± S.E.M. for 10-45 individual oocytes and data were fitted to the equation for cooperative inhibition using FigSys as described in Methods. The derived values for $K_{0.5}$ and the Hill Coefficient (n) are indicated on each plot (± S.E. of the fit shown).

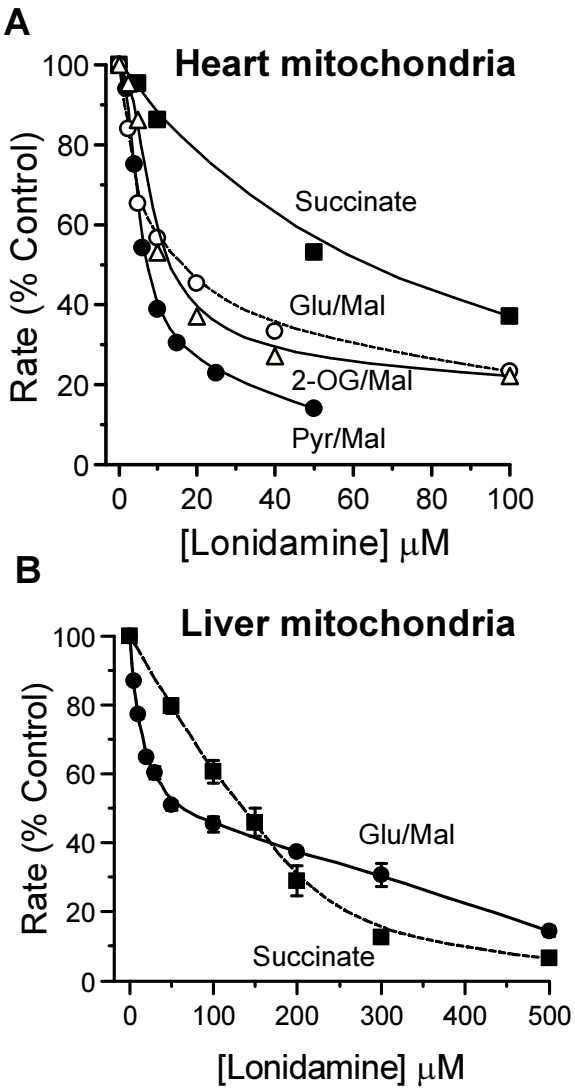

Figure 3 Lonidamine inhibits oxidation of glutamate, 2-oxoglutarate and succinate by uncoupled rat heart and liver mitochondria less potnetly than pyruvate transport
Rates of oxidation by isolated rat heart (**A**) or liver (**B**) mitochondria at 30°C were measured using an oxygen electrode as described under Methods. Data are expressed as the percentage of rates in the absence of LND to allow better comparison between the different substrates and the lines drawn were fitted by FigSys using a Bezier Spline function. For heart mitochondria, data are presented for a single representative experiment with absolute rates of pyruvate + malate, glutamate + malate, 2-oxoglutarate + malate and succinate + rotenone oxidation in the absence of LND of 84, 83, 67 and 212 nmol O_2 . min^{-1} per mg protein , respectively. For liver mitochondria (B), mean data (± S.E.M.) are presented for 3 separate mitochondrial preparations. The absolute rates of glutamate + malate and succinate (+ rotenone) oxidation in the absence of LND were 67.9 ± 3.0 and 109 ± 7.8 nmol O_2 . min^{-1} per mg protein, respectively.

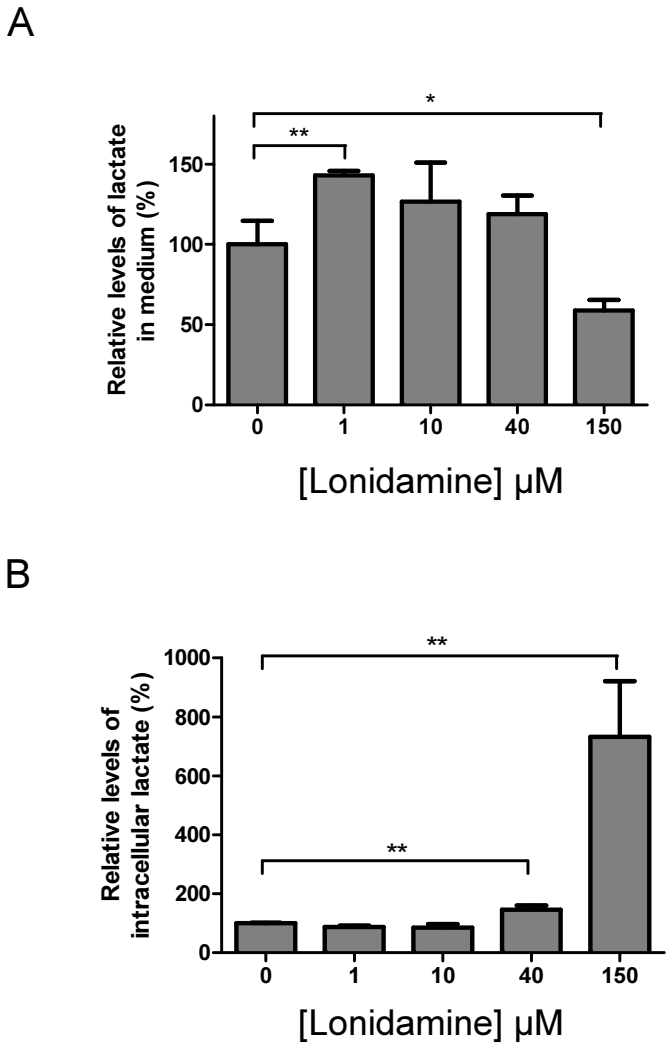

Figure 4 Concentration dependence of lonidamine effects on DB-1 melanoma cell L-lactate output and intracellular [L-lactate].
DB-1 cells were incubated with DMSO or LND at the indicated concentrations for 1 h. Levels of [L-lactate] in the culture medium (**A**) and intracellular [L-lactate] (**B**) were determined by LC-MS as described under Methods. The levels of [L-lactate] in the LND-treated group were normalized to the levels in DMSO controls. Data are presented as Means ± S.D. for 3 samples.